RSC Advances

Earth-abundant and low-cost CZTS solar cell on flexible molybdenum foil

Yongzheng Zhang[a,b], Qinyan Ye[b], Jiang Liu[b], Hao Chen[b], Xulin He[b], Cheng Liao[b*],

Junfeng Han[b], Hao Wang[a], Jun Mei[b], WoonMing Lau[b]

[a] The College of Materials Science and Engineering, Beijing University of

Technology, Beijing 100124, PR China

[b] Chengdu Green Energy and Green Manufacturing Technology R&D Centre,

Southwest Airport Economic Development Zone, Shuangliu, Chengdu, 610207, P. R.

China

* Corresponding author: Tel: +86-28-67076209, Fax: +86-28-67076210

E-mail address: cliao315@hotmail.com (Cheng Liao)

Abstract: Flexible Cu_2ZnSnS_4 (CZTS) solar cell absorbers were prepared by

sulfurizing Cu-Zn-Sn precursors which were co-electrodeposited on Mo-coated

molybdenum foil in a one-step process. Photovoltaic device with 3.82% conversion

efficiency based on the illumination area of 0.35 cm^2 was attained, which is the first

efficiency report of flexible CZTS-based solar cells on molybdenum foil.

Thin film solar cells based on copper zinc tin sulfide (Cu_2ZnSnS_4, CZTS) have

demonstrated significant improvements over recent years.[1-4] It is regarded as a

promising candidate of next generation PV material because of its high theoretical

efficiency, low-cost potential and environmental friendliness. These advantages are

based on its large absorption coefficients ($>10^4$ cm^{-1}), ideal direct band-gap (1.45 eV)

and its earth-abundance, as well as being almost free of rare or toxic elements. The

best CZTS solar cell (pure sulfide) so far, reaching 8.4% power conversion efficiency, is produced on rigid glass substrate by vacuum thermal evaporation process.[5] However, solar cells on flexible substrates seem more attractive for their applications on both ground and space utilities due to its high power/mass (W/kg) ratio, as well as further cost reduction by roll-to-roll deposition method.[6, 7]

The most commonly used flexible substrates are metal foils (e.g., stainless steel, aluminum, or molybdenum,.) and organic films (e.g., polyimide,).[8] However, the maximum sustainable temperature of polyimide (PI), typically below 500 $^\circ$C, is much lower than that of metal foils, which can withstand temperature of up to 600 $^\circ$C or even higher. Metal foils possess some distinct advantages not only in the higher temperature resistance but also in the mechanical strength over PI.[9, 10] Particularly, the high conductivity of metal foils substrate contributes to electrochemical deposition method, which is one of the best choices of low cost, low energy consumption and roll-to-roll production.[11] Among these kinds of metal foils, molybdenum is the first choice for its compatible coefficient of linear thermal expansion (linear CTE), 5.2×10^{-6} K^{-1}.[12] Besides, high purity molybdenum foil does not need the barrier layers in cell structure, whereas other substrates such as stainless steel contains some deep level impurities like Fe, which adversely affects the electronic properties of absorbers.[13]

In this work, we report an approach to fabricate CZTS films on commercial molybdenum foil by electrochemical deposition. After the CZTS device was finished with a structure of Mo foil/Mo film/CZTS/CdS/ZnO/Al:ZnO/Al, an efficiency of 3.82%

with device area of 0.35 cm^2 is attained. To our best knowledge, this is the first report of flexible CZTS-based solar cells on molybdenum foil.

Molybdenum foil (0.5 mm thick, 99.95% purity) was potentiostatically polished at 6 V (vs. Ag/AgCl) at room temperature for 1.5 min in 87.5 ml methanol and 12.5 ml sulfuric acid mixed solution. The surface morphology of post-polished molybdenum foil was analyzed using atomic force microscopy (AFM) as shown in Fig. S1 (see Supplementary Information). Then, 800 nm-thick Mo back contacts were deposited by DC sputtering (sheet resistance 0.2~0.3 Ω/square). The Cu-Zn-Sn precursors were electrodeposited in one-step process by differential pulse voltammetry method. A three-electrode system was used with Mo coated molybdenum foil as working electrode, a platinum (Pt) gauze as counter electrode and Ag/AgCl as reference electrode. Analytical reagent grade chemicals (Sigma–Aldrich) were used for the electrolytic bath preparation. The electrolyte contained 4mM $CuSO_4$, 3mM $ZnSO_4$, and 3mM $SnSO_4$ without complexing agent. The CZTS absorber layers were prepared by rapid thermal processing (RTP) the Cu-Zn-Sn precursors at 550 ^{o}C in a quartz tube filled with a 30 Torr of 5% H_2S (in N_2) for 1h. The rest of the device structure consists of 80~100 nm CdS by chemical bath deposition, ~80 nm i-ZnO/~600 nm Al-doped ZnO by RF magnetron sputtering and Ni-Al metal grids. Finally, a mechanical scribing step defined the cell area to 0.35 cm^2.

It can be seen from the cross-sectional SEM image of the precursors in Fig. 3(a) that a "flower-like" structure of Cu-Zn-Sn alloys, assembled by nano-metals with the size of approximate 40 nm, was prepared. This "flower-like" structure tends to form

homogeneous CZTS films more efficiently than ordinary structures during annealing.
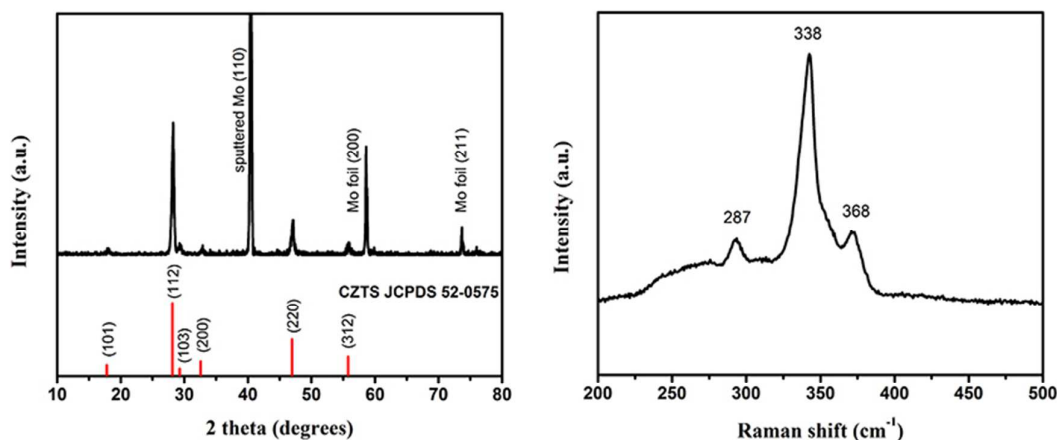
Fig.1 XRD patterns (a) and Raman spectra (b) of CZTS film.

After being annealed at 550 ^{o}C for 1h in H$_2$S atmosphere, the phase of the CZTS film were determined by XRD and Raman.Fig. 1(a) shows the XRD patterns of the CZTS absorber layer, exhibiting the main diffraction peaks of kesterite CZTS (JCPDS# 26-0575), with the lattice constants a = b = 5.427 Å and c = 10.848 Å. The sharp peaks indicate a relatively large grain size and good crystallization. The sputtered Mo (JCPDS# 42-1120) exhibits (110) crystal orientation compared to the molybdenum foil (JCPDS# 42-1120) (200), (211), which are labeled in the XRD patterns. Due to very similar lattice parameters or analogous pattern features for cubic ZnS, tetragonal Cu$_2$SnS$_3$ and kesterite CZTS, Raman spectroscopy was used to further distinguish the CZTS phase and other secondary phases. The Raman spectra shown in Fig. 1(b) verify the good purity of the kesterite CZTS phase more concretely, with the characteristic peaks at 287, 338, 368 cm^{-1}, in good agreement with well-known vibrational characteristics of CZTS material.[14, 15]
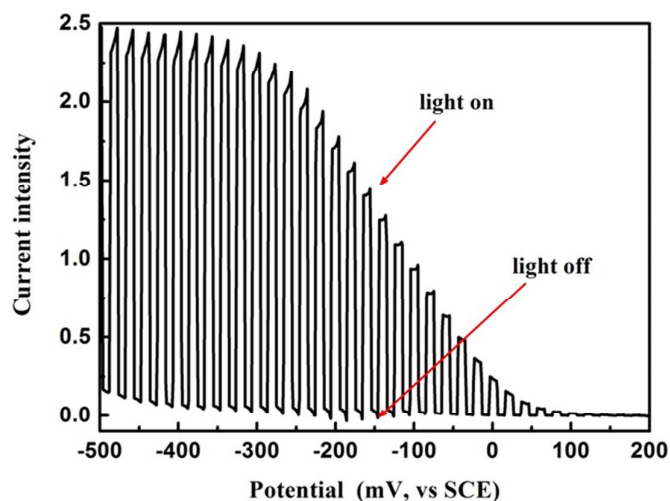
Fig. 2 Linear sweep voltammograms (LSVs) of theCZTS film.

In order to determine the photoelectric properties of the CZTS films, photoelectrochemical (PEC) measurements were carried out as shown in Fig. 2. A sharp and rapid current response arose when light was turned on, indicating that the CZTS film is sensitive to photons injection. The respectable signal at 0V also shows the light generated charge carriers have relatively long diffusion lengths (or lifetimes) to be collected without the assistance of CZTS/buffer built-in field or additional bias. This result implies the electron-hole recombination is well suppressed, which is attributed to good quality of CZTS absorber film with high crystallization and few secondary phases.
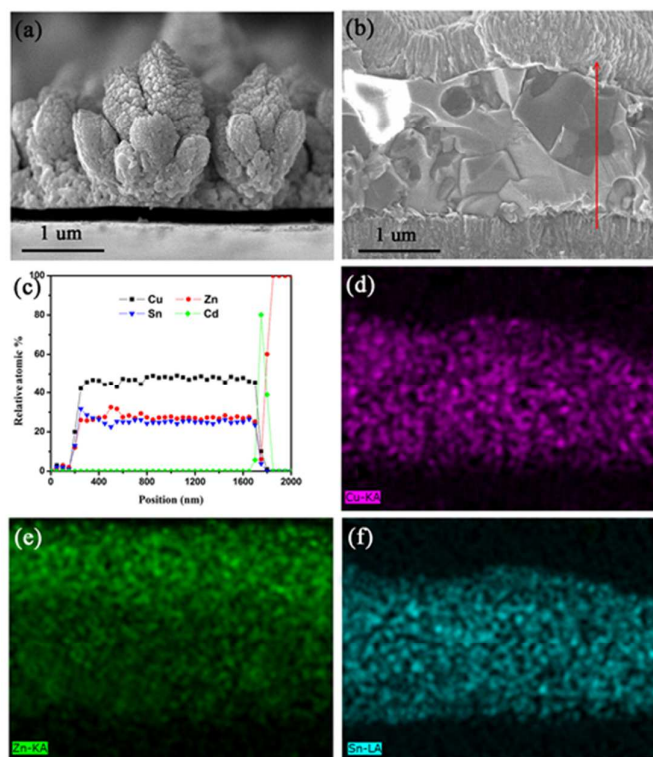
Fig.3 (a) Cross section of Cu-Zn-Sn precursors on molybdenum foil; (b) cross section of CZTS film with corresponding EDS line scan (c) taken along the red line; mapping images of Cu (d), Zn (e), Sn (f).

Fig. 3(b) presents a cross-sectional SEM image of our CZTS solar cell. The cross-section EDS elemental profiles determined from line scan and elemental mapping images are shown in Fig. 3(c) and Fig. 3(d), 3(e), 3(f), respectively. However，conventional EDS is not capable of providing quantification for the content of S due to the fact that the X-ray emission lines of Mo and S are superimposed. The X-ray emission lines are 2.29 keV for the Mo L_α line and 2.30 keV for the S K_α line. So in this case, we deducted Mo and S content and only determined Cu, Zn, Sn, and Cd. It can be learned in Fig. 3(b) that the metal elements are distributed homogeneously across the cross-section region, which indicates there is few

secondary phases such as Cu_3SnS_4 and ZnS formed during the preparation of CZTS film. On the basis of elemental profiles determined from EDS line scan as shown in Fig. 3(c), we can learn that the fluctuation of homogeneity throughout the bulk of the film is tiny. The ratios of Cu/Zn+Sn and Zn/Sn calculated from Fig. 3(c) are 0.82~0.85 and 1.2~1.3, respectively, yielding Cu-poor and Zn-rich compositions. The grain nucleation and growth of CZTS films out of initially Cu-poor and Zn-rich environments, just like the case in this work, is significant to the formation of intrinsic defects, including V_{Cu} vacancies, Zn_{Cu} antisites and derivative defect clusters. These intrinsic defects act as shallow acceptors and show p-type conductivity, according to some works based on first principle calculations.[16]

Table 1 Characteristics of other devices

Cell	V_{oc} / mV	J_{sc} / mA•cm^{-2}	FF / %	Rs / Ω•cm^2	Eff. / %
D1	497	15.05	46.3	4.32	3.46
D2	442	15.56	38.9	6.23	2.68
D3	422	11.87	47.4	4.40	2.37
D4	454	11.03	42.3	4.87	2.12
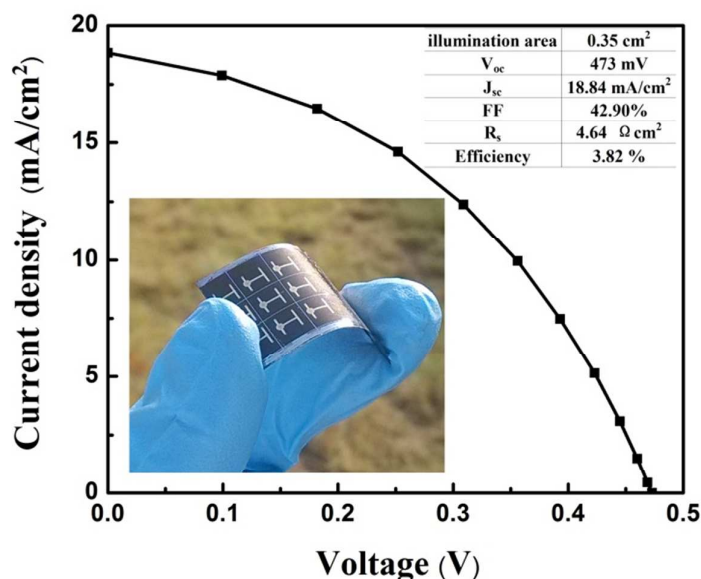
Fig. 4 *J-V* curve of the best CZTS solar cell measured under a simulated AM1.5G illumination. The inset is photograph of a sample on molybdenum foil with single cells.

Table 1 shows the characteristics of other devices and Fig. 4 shows the *J-V* characteristics for the best flexible CZTS solar cell under AM1.5G illumination. The best device represents a power conversion efficiency (PCE) of 3.82% with the illumination area of 0.35 cm^2, which is the first efficiency report of flexible CZTS based solar cells on molybdenum foil so far. The device gives an open circuit voltage of V_{oc} = 473 mV and photocurrent of J_{sc} = 18.84 mA/cm^2 where the fill factor (FF) is 42.90%. The present CZTS cell has relatively lower J_{sc} and higher V_{oc}, compared with our previous work.[17] The PCE may be limited by a high series resistance (4.64 Ωcm^2), resulting in a substantial loss in fill factor. It is expected that a significant improvement in device performance could be achieved by improving the sheet resistances of the Mo and AZO layers. In addition, the interface defects or bulk defects near the CZTS/CdS heterojunction would impact the carrier lifetime, which

cause the decrease of V_{oc} significantly. Besides, reflection by the metal contacts or the active area of the device, as well as absorption of CdS buffer layer and transparent conducting oxide layer, could decrease J_{sc}.
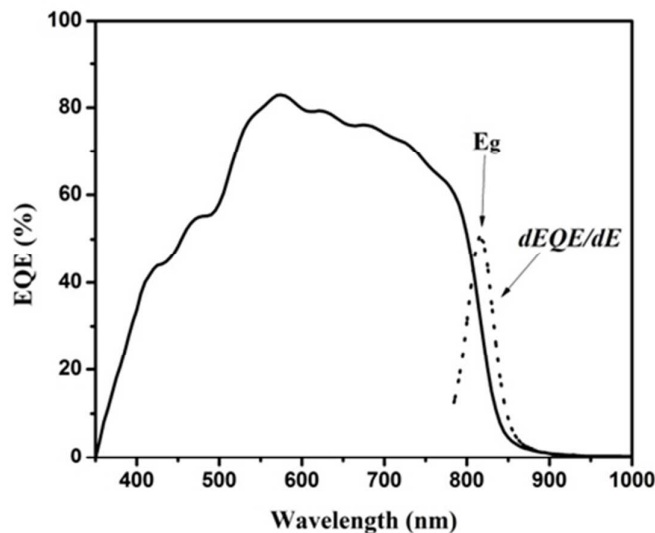
Fig. 5 External quantum efficiency (EQE) curve of ZnO/CdS/CZTS heterojunction solar cell. The insert is the derivative of EQE as a function of wavelength.

The external quantum efficiency (EQE) curve of the corresponding ZnO/CdS/CZTS heterojunction solar cell is presented in Fig. 5. The EQE starts slowly at about 400 nm due to the cut-off of CdS buffer layer and ZnO window layer. The quantum efficiency reaches a maximum value of 82.9% at 575 nm. However, it drops off significantly in the near-IR range and ends around 900nm, which is related to optical absorption of the CZTS absorber. The dotted line inserted is the derivative of EQE as a function of wavelength, which is used to estimate the effective band gap of the absorbers. Peak at 820 nm is observed in the dotted curve, corresponding to

absorption edges of CZTS films. According to the inverse correlation between photon energy and wavelength, the band gap of CZTS absorber can be calculated to be 1.51 eV from the peak at 820 nm. Assuming there is no optical and electrical loss from ZnO or CdS layers, and 100% quantum efficiency is attained between 350 nm and 510 nm, the J_{sc} would rise to 25.2 mA/cm^2, which is still far lower than the typical J_{sc} of the CZTSe solar cell (~35 mA/cm^2). Although the open-circuit voltage is higher than most CZTSe cells, which have wider band gaps, the value of V_{oc} does not increase proportionally with the increase of the band-gap energy, thus decreasing the conversion efficiency as compared with our previous results. Achieving a higher efficiency appears to be limited by a V_{oc} deficit and low fill factor in addition to a rather high series resistance of 4.64 Ωcm^2. Besides, broadening the spectrum absorption range by decreasing the absorber band-gap and simultaneously maintaining the existing V_{oc} would help to improve efficiency. Improvements in device performance are expected with further studies by optimization of the absorber band-gap with Se partly replacing S.[1] Thinning the thickness of CdS and TCO layers and increasing CZTS layer to make sure the maximizing the light transmission into the CZTS absorber layer is also a way to increase J_{sc}.[3]

In summary, we report a method to fabricate CZTS solar cells on flexible molybdenum foil with power conversion efficiency of 3.82% based on the illumination area of 0.35 cm^2. From the data of EQE, Further optimization of synthesis and device fabrication would lead to enhanced efficiency and a high power/mass ratio route to earth-abundant elements, low-cost, widely-used thin film

solar cells. However, further improvement requires extensive systematic investigations to optimize the involved layers and processing conditions.

Acknowledgements

References

1. W. Wang, M. T. Winkler, O. Gunawan, T. Gokmen, T. K. Todorov, Y. Zhu and D. B. Mitzi, *Advanced Energy Materials*, 2013, DOI: 10.1002/aenm.201301465, n/a-n/a.
2. K. Ramasamy, M. A. Malik and P. O'Brien, *Chemical Communications*, 2012, 48, 5703.
3. M. T. Winkler, W. Wang, O. Gunawan, H. J. Hovel, T. K. Todorov and D. B. Mitzi, *Energy & Environmental Science*, 2014, DOI: 10.1039/C3EE42541J.
4. A. Polizzotti, I. L. Repins, R. Noufi, S.-H. Wei and D. B. Mitzi, *Energy & Environmental Science*, 2013, DOI: 10.1039/c3ee41781f.
5. B. Shin, O. Gunawan, Y. Zhu, N. A. Bojarczuk, S. J. Chey and S. Guha, *Progress in Photovoltaics: Research and Applications*, 2011, DOI: 10.1002/pip.1174, n/a-n/a.
6. A. Chirila, S. Buecheler, F. Pianezzi, P. Bloesch, C. Gretener, A. R. Uhl, C. Fella, L. Kranz, J. Perrenoud, S. Seyrling, R. Verma, S. Nishiwaki, Y. E. Romanyuk, G. Bilger and A. N. Tiwari, *Nature materials*, 2011, 10, 857-861.
7. N. G. Dhere, *Solar Energy Materials and Solar Cells*, 2007, 91, 1376-1382.
8. F. Kessler and D. Rudmann, *Solar Energy*, 2004, 77, 685-695.
9. D. Rudmann, D. Brémaud, H. Zogg and A. Tiwari, *Journal of Applied Physics*, 2005, 97, 084903.
10. R. Caballero, C. A. Kaufmann, T. Eisenbarth, T. Unold, R. Klenk and H. W. Schock, *Progress in Photovoltaics: Research and Applications*, 2011, 19, 547-551.
11. A. Kampmann, J. Rechid, A. Raitzig, S. Wulff, M. Mihhailova, R. Thyen and K. Kalberlah, *Materials Research Society Symposium Proceedings,* 2003, 763, 323-328,.
12. M. Patel and A. Ray, *Physica B: Condensed Matter*, 2012, 407, 4391-4397.
13. K. Herz, A. Eicke, F. Kessler, R. Wächter and M. Powalla, *Thin Solid Films*, 2003, 431, 392-397.
14. A. Shavel, D. Cadavid, M. Ibáñez, A. Carrete and A. Cabot, *Journal of the American Chemical Society*, 2012, 134, 1438-1441.
15. E. Thimsen, S. C. Riha, S. V. Baryshev, A. B. F. Martinson, J. W. Elam and M. J. Pellin, *Chemistry of Materials*, 2012, 24, 3188-3196.
16. S. Chen, A. Walsh, X. G. Gong and S. H. Wei, *Adv Mater*, 2013, 25, 1522-1539.
17. Y. Zhang, C. Liao, K. Zong, H. Wang, J. Liu, T. Jiang, J. Han, G. Liu, L. Cui, Q. Ye, H. Yan and W. Lau, *Solar Energy*, 2013, 94, 1-7.

illumination area	0.35 cm^2
V_{oc}	473 mV
J_{sc}	18.84 mA/cm^2
FF	42.90%
R_s	4.64 Ω cm^2
Efficiency	3.82 %
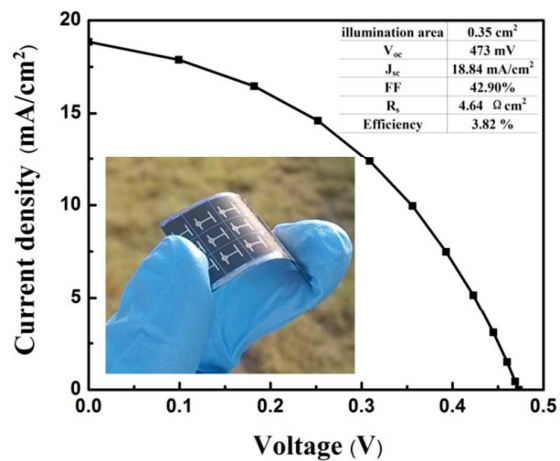
Flexible Cu$_2$ZnSnS$_4$ (CZTS) solar cell with 3.82% conversion efficiency is prepared by co-electrodeposited method.